Ecological Indicators 128 (2021) 107831

Contents lists available at ScienceDirect

Ecological Indicators

journal homepage: www.elsevier.com/locate/ecolind

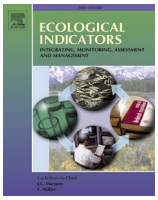

Strength of association between vegetation greenness and its drivers across China between 1982 and 2015: Regional differences and temporal variations

Huan Wang [a,b], Shijie Yan [c], Ze Liang [a,b], Kewei Jiao [d], Delong Li [a,b], Feili Wei [a,b], Shuangcheng Li [a,b,*]

[a] College of Urban and Environmental Sciences, Peking University, Beijing 100871, China
[b] Key Laboratory for Earth Surface Processes of The Ministry of Education, Peking University, Beijing 100871, China
[c] Aerospace Information Research Institute, Chinese Academy of Sciences, Beijing 100094, China
[d] Key Laboratory of Forest Ecology and Management, Institute of Applied Ecology, Chinese Academy of Sciences, Shenyang 110016, China

ARTICLE INFO

Keywords:
Vegetation greenness
Regional difference
Temporal dynamic
Quantitative attribution
Strength of association
GeoDetector method

ABSTRACT

Analysis focused on sub-regional differentiation of vegetation greenness and their dominant drivers are needed to properly develop targeted strategies for sustainable management. In this study, we took China as a case study area, and analyzed the spatiotemporal heterogeneity of vegetation greenness and its strength of association with both environmental (topographical factors and hydrothermal conditions) and anthropogenic factors (land use type and population density) across six eco-geographic regions during 1982–2015. The whole period was divided into two periods by the turning point of 1998, after which China has implemented numerous forest protection projects. The attribution results based on the Geodetector method show the followings: (1) In China, precipitation is the dominant factor in landscape variation of Normalized Difference Vegetation Index (NDVI) with a strength of association of 85%. Additionally, precipitation is also the dominant factor in arid and semi-arid regions, including Northern semiarid (NS) region, Northwestern arid (NWA) region and Qinghai-Tibet Plateau (QTP) region. The dominant factors differ across diverse eco-geographic regions; for example, slope dominates in sub-tropical/tropical humid (STH) and middle temperate humid/sub-humid (MTH) regions. (2) Generally, the strength of association between vegetation and temperature decreases across China over the past 34 years, meaning that the limiting effect of temperature on the NDVI is weakened, similarly, the controlling effect of water conditions is also weakened. In contrast, the spatial association between anthropogenic factors and NDVI is enhanced. (3) The temporal dynamics of strength of association between factors and the NDVI differ in diverse periods and regions; for example, the strength of association between wind speed and NDVI decreased during 1982–1998, but increased during 1999–2015 in temperate humid/sub-humid (WTH) region; however, decreasing trends were revealed in the QTP region in both periods. Our study highlights that variation of NDVI is mainly attributed to climate change and land cover change. Generally, the limiting impact of hydrothermal conditions on NDVI weakens, and the controlling effect of human activity increases over time.

1. Introduction

Vegetation, as a sensitive indicator of climate change and pivotal link in land atmosphere interactions (Liu and Lei, 2015), plays an important role in regulating the interchange of water and heat fluxes, soil ecosystems and carbon and nitrogen cycles (Bonan, 2008; Fu et al., 2017; Qu et al., 2020). Previous research revealed that global tree cover increased by 7.1% in 2016 relative to 1982, and land-cover change displayed regional differences, such as tropical deforestation and temperate afforestation (Song et al., 2018). China and India dominated the greening of the world, and the greening was mostly attributed to land-use management (Chen et al., 2019). Although there is increasing attention to identifying the spatial patterns and dominant factors relevant to vegetation greenness and their relative contributions (Liu and

* Corresponding author.
E-mail addresses: 2001111811@stu.pku.edu.cn (H. Wang), yansj@radi.ac.cn (S. Yan), liangze@pku.edu.cn (Z. Liang), jiaokewei@iae.ac.cn (K. Jiao), dlli@pku.edu.cn (D. Li), weifeili@pku.edu.cn (F. Wei), scli@urban.pku.edu.cn (S. Li).

https://doi.org/10.1016/j.ecolind.2021.107831
Received 15 June 2020; Received in revised form 8 May 2021; Accepted 11 May 2021
Available online 31 May 2021

Lei, 2015; Wang et al., 2016b; Chen et al., 2019), the differentiation of influencing mechanisms on vegetation dynamics at sub-regional scales across one region still needs to be more explored and documented.

China accounts for 25% of the global net increase in leaf area, namely increase in greenness, with only 6.6% of global vegetated area, attributed to the combined effect of climate change and ambitious engineering projects related to conserve and expand forests, such as 'Grain for Green' project (Chen et al., 2019; Zhao et al., 2020). However, the multiple factors that control distribution of vegetation, as well as their recent dynamics display high spatial heterogeneity across regional and sub-regional land surfaces (Gao et al., 2019), indicating the response of vegetation to environmental factors may differ from region to region. Evidence has shown that surface greenness patterns are triggered by heterogeneous mechanisms over different regions. For example, Nemani et al. (2003) found that water availability was the main limiting factor in vegetation growth for over 40% of earth's vegetated surface, followed by temperature and radiation. Piao et al. (2015) suggested that rising atmospheric CO_2 concentration chiefly drove China's greening, with a contributing rate of 85% to changing trend of average growing-season LAI. Therefore, spatial heterogeneity deserves more attention for a better understanding of the drivers and landscape patterns of vegetation. In this study, eco-geographic regionalization, which provides a regional framework for studying regional differentiation and the regional response to global change across China (Zheng, 2008), was used to explore spatially heterogeneous differences in the spatial association between vegetation greenness and its influencing factors.

The influencing mechanisms of vegetation dynamics in terrestrial ecosystems are well documented over various spatiotemporal scales using remote sensing observation of vegetation indices (Fensholt et al., 2012; Zhu et al., 2016; Cai et al., 2015, 2016; Zhang et al., 2020a). Numerous publications explored the driving forces underlying the vegetation dynamics, including climate constraints, anthropogenic activities, topographical influences, CO_2 fertilization, nitrogen deposition and wildfire (Xiao and Moody, 2005; Niinemets et al., 2011; Buitenwerf et al., 2012; Piao et al., 2015; Huang et al., 2018; Kalisa et al., 2019; Gao et al., 2019; Leverkus et al., 2019). For example, Huang et al. (2020) indicated a stronger effect of climate change (about 59.3%) than human activities in the Beiluo River Basin using a support vector machine based simulation model. Lü et al. (2015) applied correlation and comparative analysis to determine the driving forces for vegetation change (socio-economic and climate factors were included) and confirmed that socioeconomic factors, such as human population and economic production, were the most significant factors for vegetation change. Although these studies identified the dominant driving forces for vegetation greenness, a comprehensive comparison of the relative importance of multiple factors for vegetation greenness is still not well understood. In this study, GeoDetector method, will be used to evaluate the relative importance among diverse drivers. This method is good at the analysis of categorical variables, making it convenient and available to compare the relative importance of categorical and continuous variables (Wang and Xu, 2017).

The response of vegetation to environmental perturbations and changes is complex and nonlinear due to the interactions among multiple factors (Piao et al., 2015; Zhao et al., 2015; Gao et al., 2017). Several studies have documented the nonlinear, concave-down relationships between regional precipitation and aboveground net primary production (Huxman et al., 2004; Yang et al., 2008; Hsu et al., 2012). Nonlinear influences and interactions make it challenging to quantify the contribution of each relevant factor to vegetation greenness (Piao et al., 2020). The GeoDetector method is a nonlinear analysis method based on variance analysis and the spatial distribution consistency between two factors with a causal relationship. The core assumption is that if one factor influences and is correlative with another, their spatial distributions must be similar to some degree; no matter whether the relationship is linear or nonlinear, the relationship can be detected (Wang et al., 2010). In this study, climatic factors, anthropogenic factors, and topographic factors are considered as drivers for vegetation greenness in the quantitative attribution analysis. NDVI is used as the metric of vegetation greenness, which has been broadly used in the research of changes in vegetation greenness and the response of vegetation to climate change and anthropogenic activity across diverse spatiotemporal scales (Wang et al., 2011; Krishnaswamy et al., 2014; Tao et al., 2015; Du et al., 2017; Zhang et al., 2020b).

Against the background of climate change and severe anthropogenic activities, the relationship between vegetation greenness and environmental limitations may have changed over time (Piao et al., 2014). For example, Keenan and Riley (2018) quantified the spatial functional response of vegetation cover to temperature and confirmed that the temperature limitation had declined over time, which was consistent with expectations based on recent warming. Piao et al. (2006) pointed out that the impact of rising temperature on the current enhanced greening trend will decline or even disappear. However, the temporal dynamics of the impact of influencing factors on vegetation greenness are still poorly understood; clarifying the changing trend in the strength of association between factors and vegetation greenness is vital in predicting the response of vegetation to climate change and human disturbance, and thus in creating adaptive strategies.

There is a need to explore the spatial differences and temporal dynamic of the strength of association between influencing factors and vegetation greenness. The primary objectives of this paper are to (1) quantify the heterogeneous landscape variation in NDVI and its changing trend across different eco-geographic regions in China during 1982–2015; (2) detect the dominant factors in vegetation greenness and their relative importance; (3) explore the temporal changing trends of strength of association between the influencing factors and NDVI.

2. Method

2.1. China's eco-geographic regions

China's eco-geographic regionalization was demarcated or combined with different elements based on regional differentiation of the earth's surface, in which temperature and air moisture condition were considered in first level division (Zheng, 2008). Eco-geographic regionalization was widely used in the assessment of terrestrial ecosystems across China (Wu et al., 2010; Zhao and Wu, 2014). The first-level contains eight zones, including cold temperate humid (CTH) region, middle temperate humid/sub-humid (MTHS) region, north semi-arid (NS) region, warm temperate humid/sub-humid (WTH) region, sub-tropical humid (SH) region, tropical humid (TH) region, northwest arid (NWA) region, and Qinghai-Tibet Plateau (QTP) region. Due to the areas of CTH region and TH region are small in China (Fig. S1a), further the less sample points fail to acquire an accurate attribution results of vegetation greenness. Thus, we have merged the eight regions into six regions, the CTH region and MTHS were integrated to cold/ middle temperate humid/sub-humid (MTH) region, and the SH and TH region were integrated to sub-tropical/tropical humid (STH) region (Fig. S1b). Six top-level regions were considered in this study: MTH region, NS region, WTH region, STH region, NWA region, and QTP region (Fig. 1). The topography (Fig. 1a), temperature (Fig. 1b), precipitation (Fig. 1c) and land use type (Fig. 1d) were highly heterogeneous in different eco-geographic regions, in which temperature and precipitation were the means over the length of the study period. The mean value of geographic environmental factors in diverse eco-geographic regions differed a lot (Table 1), such as the difference of mean temperature between the STH and QTP region reached 17℃, and the mean precipitation in STH was approximately 8.9 times higher than that in NWA. In the MTH and STH regions, nearly half of the area was occupied by forest land; in the NS and QTP regions, grassland is distributed in most areas; and dry land and unused land were the dominant land use types with area ratio of 50.93% and 62.15% in the WTH and NWA regions respectively (Table S1). Due to lack of availability of data, the islands of China were not included in

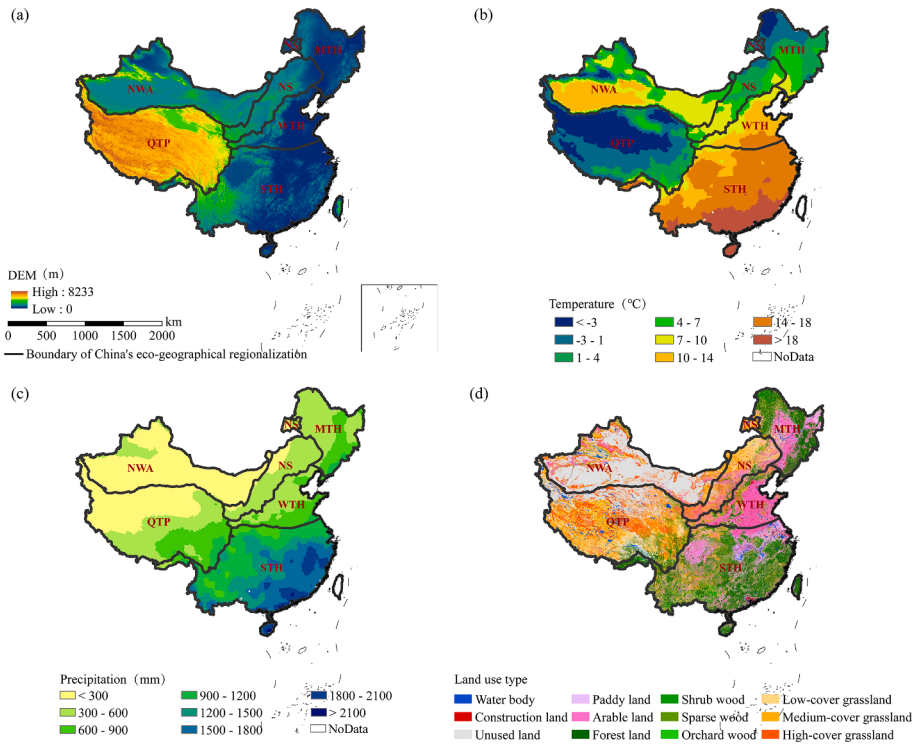

Fig. 1. Studied eco-regions in China. (a) Elevation, (b) Mean temperature during 1982–2015, (c) Mean precipitation during 1982–2015, (d) Land use type in 2015 (Note: The acronyms of each region show in study area section.).

Table 1
Mean value of geographic environmental factors in different eco-geographic regions.

Region	MTH	NS	WTH	STH	NWA	QTP
Elevation (m)	416.41	1145.57	508.61	772.21	1427.81	4464.67
Precipitation (mm)	578.29	375.15	622.60	1335.46	150.19	400.23
Relative humidity (%)	66.59	55.37	64.07	77.20	46.85	47.54
Mean temperature (℃)	1.88	4.59	11.27	16.00	7.33	−1.66
Maximum temperature (℃)	8.31	11.41	17.21	21.04	14.60	5.71
Minimum temperature (℃)	−3.91	−1.34	6.35	12.44	0.91	−7.85
Wind speed (m/s)	2.64	2.99	2.23	1.84	2.78	4.01

the quantitative attribution analysis, including the South China Sea islands and Taiwan island.

2.2. Data sources

We used the biweekly NDVI dataset from Global Inventory Modeling and Mapping Studies (GIMMS) for the period 1982–2015, with a spatial resolution of 0.083°. The GIMMS NDVI dataset is corrected through a series of processing steps to reduce limitations of AVHRR (Advanced Very-High-Resolution Radiometer) measurement arising from calibration, view geometry and volcanic aerosols, and the dataset has been verified using stable desert control points (Zhou et al., 2001). The AVHRR GIMMS NDVI (version 3 g.v1) datasets are available at https://ecocast.arc.nasa.gov/-data/pub/gimms/3g.v1/.

The climate data of hydrothermal factors used in this study included daily precipitation; humidity; wind speed; and maximum, mean and minimum temperature with a spatial resolution of 0.25° during 1982–2015, downloaded from the National Meteorological Information Center (http://data/cma.cn). The land use type data for 1980, 1990, 1995, 2000, 2005, 2010, and 2015, the boundary of the eco-geographic region and digital elevation model (DEM) with spatial resolution of 1-km were acquired from the Data Center for Resources and Environmental Sciences, Chinese Academy of Sciences (http://www.resdc.cn). The population density data with 1-km spatial resolution during 2000–2015 were acquired from the LandScan global population database developed by Oak Ridge National Laboratory (https://landscan.ornl.gov); the population density data (1-km resolution) for 1990 were downloaded from the Data Center for Resources and Environmental Sciences, Chinese Academy of Sciences (http://www.resdc.cn).

2.3. Methods

2.3.1. Trend analysis

In assessing vegetation variability for each pixel across the entire study area, we used a least-squares linear regression model given by Eq. (1):

$$y_t = a + bx_t + \varepsilon \quad (1)$$

where y_t and x_t are the NDVI time series and time span, respectively; a and b represent the regression intercept and slope, respectively, for the linear model; and ε is the residual error of the fit. The slope (b) of the regression indicates the temporal changing trend, namely the variability over time—for b greater than 0 the trend increases, and for $b < 0$ the trend decreases. Significance was quantified using an F-test. We selected p-value of<0.1 to test significance of changing trend, only significant pixels were displayed in Fig. 2.

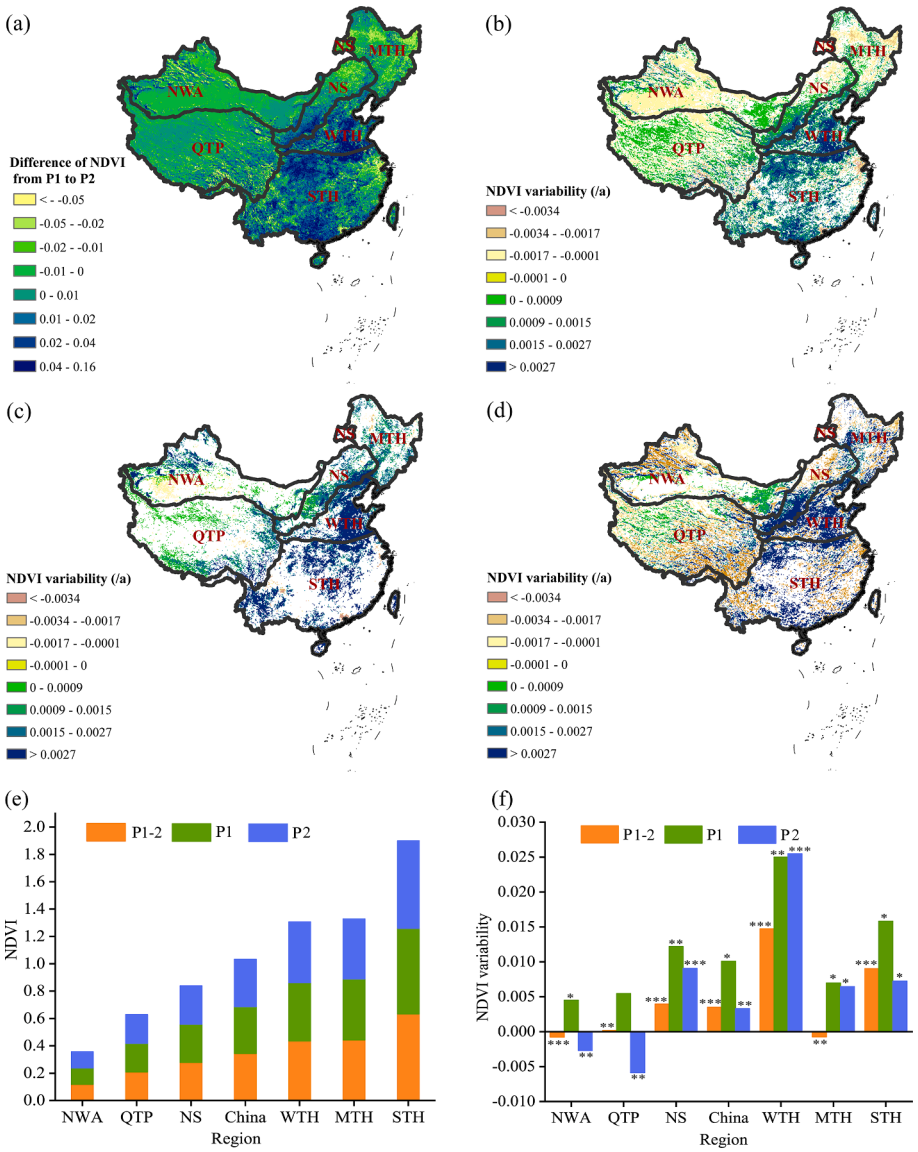

Fig. 2. The statistics of NDVI and its variability. (a) Difference of NDVI from P1 to P2, (b) NDVI variability with significance (p value < 0.1) in P1-2, (c) NDVI variability with significance (p value < 0.1) in P1, (d) NDVI variability with significance (p value < 0.1) in P2, (e) mean value of NDVI, (f) mean variability (/10a) of NDVI (*** means p value < 0.01, **means p value < 0.05, * means p value < 0.1).

2.3.2. *Turning point (TP) identification based on the piecewise regression model*

In order to detect the potential TP of the NDVI time-series trend, we applied a piecewise regression model (Toms and Lesperance, 2003), which is widely used in the TP detection of NDVI (Sun et al., 2011; Piao et al., 2011). The premise of this study is that changes in greenness vary spatially, thus TP detection was based on a national scale. The equations are as follows:

$$y = \begin{cases} \beta_0 + \beta_1 t + \varepsilon, & t \leqslant \alpha \\ \beta_0 + \beta_1 t + \beta_2 (t - \alpha) + \varepsilon, & t > \alpha \end{cases} \quad (2)$$

where y and t are the NDVI and year, respectively; α is the estimated TP of the time-series trend change; β_0, β_1, β_2 are regression coefficients; β_0 is the intercept; β_1 and $\beta_1 + \beta_2$ are the magnitudes of the trends of the two time series before and after TP; and ε is the residual error of the fit. Least-squares linear regression is used in estimating the fitted variables, with a p value < 0.05 considered as significant.

2.3.3. *GeoDetector method*

The GeoDetector method can test the spatial heterogeneity of single variable Y as well as the possible causal relationships between Y and other variables X by examining the coupling consistency of the spatial distribution of the two variables (Wang et al., 2010, 2016a). The key maxim is that if influencing factor X is associated with relevant outcome Y, then the spatial distribution of X is similar to that of Y in geographical space. If X is a continuous raster, it must be discretized into layers. The method is based on the variance analysis of Y based on the layers divided by each X factor (Fig. S2, Wang and Xu, 2017). We applied the method to identify the spatial heterogeneity and dominant factors of NDVI. Namely, Y was NDVI, and X concluded elevation, slope, precipitation, humidity, mean temperature, maximum temperature, minimum temperature, wind speed, land use type and population density in this study. The strength of association between factors and NDVI can be measured by the q value; the temporal change in this value can reflect the temporal change of strength of association between influencing factors and NDVI. The q value is defined as:

$$q = 1 - \frac{1}{N\sigma^2}\sum_{h=1}^{L} N_h \sigma_h^2 \quad (3)$$

where σ_h^2 is the variance of *NDVI* within layer *h* of influencing factor *X* ,N_h is number of sample units in layer *h*, σ^2 and *N* are the global variance of NDVI and total samples in the study area (e.g. if the detection was aimed at China, the variance and *N* were at the national scale, if the detection was based on eco-geographic zones, the variance and *N* referred to eco-geographic regions), and *L* is the number of layers of factor *X*. Higher values of *q* indicate higher spatial heterogeneity of NDVI along the *X* layer; in addition, a higher *q* value also means a higher strength of association between *X* and NDVI (Wang et al., 2016a). The significance of the *q* value can be tested by an *F*-test. The natural break method was used to discrete the X factors (Gao and Wang, 2019; Wei et al., 2020). In order to ensure the comparability of the results, the same stratification method of *X* factors was applied for diverse eco-geographic regions.

Due to the complexity of geographic processes, controlling factors often do not act independently but instead act collectively (Wang et al., 2018). The interaction detector can identify the interaction effect between two different factors *X1* and *X2*, which can be determined by the value of *q*(X1 ∩ X2) (Fig. S3, Wang and Xu, 2017). The calculation of the interaction factor needs to overlay the two classification layers *X1* and *X2* to generate a new classification variable *X1* ∩ *X2* first, and then, calculate the *q* value using equation (3). The *q* value of variable *X1* ∩ *X2* measures the interaction effect between *X1* and *X2*. If the *q*(X1 ∩ X2) is higher than *q*(*X1*) and *q*(X2), and the interaction type between two variables is enhanced. Details on the GeoDetector method can be found in Wang et al. (2010) and Wang and Xu (2017).

3. Results

3.1. Spatiotemporal dynamics of NDVI

Based on a piecewise regression model, the TP of NDVI dynamics during 1982–2015 (P1-2) was 1998 in China, which is the same year the Chinese government launched several large-scale ecological restoration projects, such as the Natural Forest Conservation Project (initiated in late 1998) and the Grain for Green Project (introduced in 1999) (Xu et al., 2006; Zhao et al., 2020). We divided the whole period into sub-periods P1 (1982–1998) and P2 (1999–2015). In China, the mean value of NDVI increased 0.004 from P1 to P2, NDVI increased mostly in south NS, WTH, and STH region (Fig. 2a, e). NDVI represents high spatial heterogeneity due to complex topographical, environmental, and anthropogenic conditions across China. NDVI is lowest in the NWA zone (mean value = 0.118) and highest in the STH zone (mean value = 0.632) in P1-2 (Fig. 2e). Although the mean NDVI variability was positive in the three periods (P1-2, P1, P2) across China (Fig. 2f), the greening and browning trends both exist across different eco-geographic regions (Fig. 2b–d). During 1982–2015, NDVI increases most significant in the WTH and STH regions and decreases in the MTH and NWA regions (Fig. 2f). The changing trend of NDVI differs across different time spans. For example, all regions display a significant increasing trend in P1, but NWA and QTP showed a significant decreasing trend in P2 (Fig. 2f).

3.2. Quantitative attribution analysis of NDVI across different regions

3.2.1. Identification of dominant influencing factors

In China, the spatial distribution of NDVI is mainly controlled by water conditions. Precipitation dominated with a *q* value of 85%, followed by humidity (*q* value = 0.81) in P1-2 (Fig. 3a). Fig. 3a shows the minimum temperature owed the larger *q* value than mean temperature and maximum temperature; land use type can explain nearly 60% of the

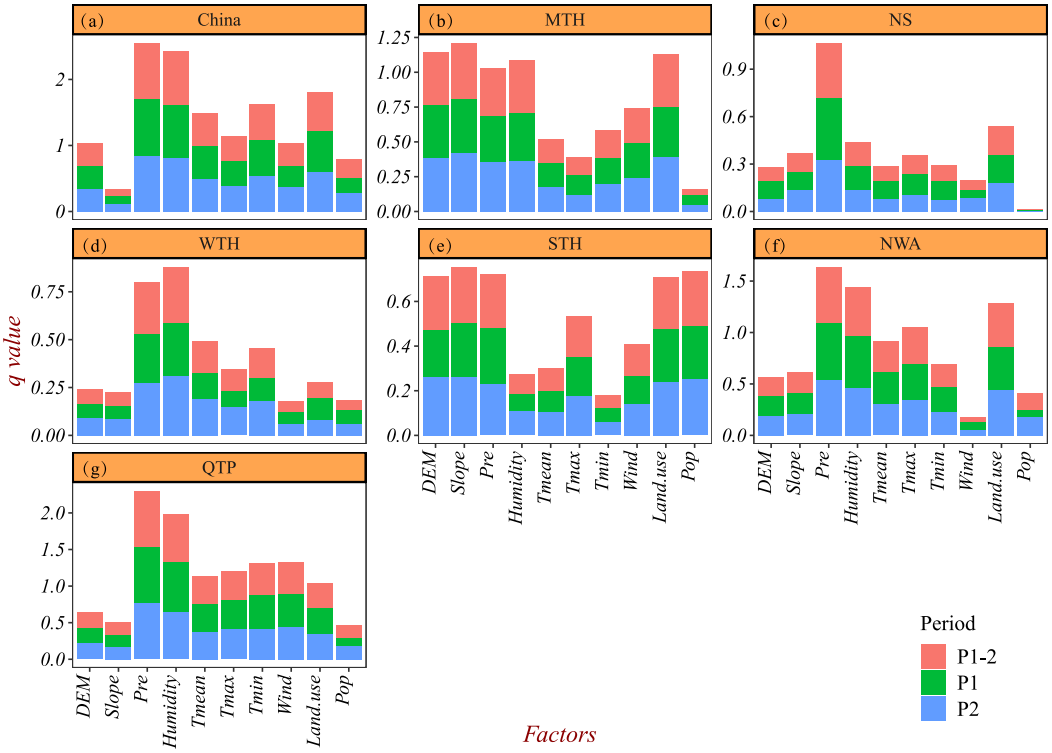

Fig. 3. The *q* value (*p* value < 0.01) of influencing factors for NDVI during the three periods across regions (note: Pop and Pre represent population density and precipitation, respectively).

NDVI distribution; the q value of population is larger in P2 than in P1 across China. From west to east, the q value of temperature decreased significantly, with the highest value in QTP region and followed by NWA region (Fig. 3). In the relatively humid regions, including MTH and STH regions, topographic factors play more important role in the spatial distribution of NDVI than that in other regions. In the arid regions, including NS and NWA regions, precipitation is the dominant factor for NDVI; the q value of the maximum temperature is larger than that of mean temperature and minimum temperature (Fig. 3c, f). In the STH region, the q values of elevation, slope and precipitation are very close, but the dominant factor with highest q values differ in diverse periods, as follows: slope in P1-2 (q value of 0.253), precipitation in P1 (q value of 0.252), and elevation in P2 (q value of 0.261) (Fig. 3e). In the QTP region, precipitation is the dominant factor followed by humidity (Fig. 3g). In general, precipitation has larger q values in arid and semi-arid regions, such as the NS, NWA and QTP regions, compared with humid regions; temperature has its highest q value in the QTP region, and population had its largest q value in the STH region; land use type has its highest values in NWA and QTP regions.

3.2.2. Identification of dominant interaction influencing factors

The interactions between two drivers often enhance their impacts on NDVI, the dominant interaction factors are identified in this study. Table 2 shows that the interaction factor between precipitation and elevation is the dominant factor for landscape variation of NDVI in China, accounting for more than 90% of the NDVI distribution. In general, in the east coast region of China, including MTH, WTH and STH regions, the dominant interaction factor is the factor between precipitation and elevation. In the arid regions with lower temperature, such as NS and QTP regions, the interaction factor between precipitation and temperature is the dominant interaction factor. In NWA region where most of the land surface was covered by unused land, the interaction factor between precipitation and land use type is the dominant factor. In addition, the dominant interaction factor may differ in different time periods. For example, the interaction between precipitation and maximum temperature is the dominant interaction factor during P1-2 and P2, and the interaction between precipitation and mean temperature is the dominant factor in P1 in the NS region. The interaction between humidity and elevation was the dominant factor in WTH in P1-2, and the interaction of precipitation and elevation in P1 and P2.

3.3. Temporal dynamics of spatial association between factors and NDVI in different regions

3.3.1. Topographic factors

From 1982 to 2015, the strength of association of elevation for NDVI significantly decreases across China (Fig. 4a) and in most sub-regions, including NS (Fig. 4g), NWA (Fig. 4p), and QTP (Fig. 4s) regions. However, the q value of elevation significantly increased in WTH (Fig. 4j) and STH (Fig. 4m) regions. The direction of change in trend differs in different periods. For example, the q value of elevation increases significantly in P1 ($P < 0.05$) (Fig. 4b), but decreases significantly in P2 ($P < 0.1$) (Fig. 4c) in China. In WTH, the q values increase in both P1 and P2 (Fig. 4k, l). The q values decrease in both P1 and P2 in MTH, NS, and NWA (Fig. 4e–f, h–i, q–r) regions. In China, the q value of slope decreases significantly in P1-2 (Fig. 4a), increases in P1 (Fig. 4b), and decreases significantly in P2 (Fig. 4c); a similar changing trend is seen in QTP (Fig. 4s–u). The q values of slope showed an increasing trend in MTH, NS, and WTH during P1-2, P1 and P2 (Fig. 4d–l); an opposite change in trend is observed in NWA (Fig. 4p–r).

3.3.2. Water conditions

Generally, the q values of water conditions show decreasing trends across different regions (Fig. 5). In China, precipitation shows decreasing trend during the three periods (Fig. 5a–c). In MTH, the q value of precipitation decreases in P1-2 and P2 (Fig. 5d, f) and increases in P1 (Fig. 5e). The q value of precipitation shows an increasing trend (Fig. 5g–i) in NS and a decreasing trend in the WTH, STH, NWA, and QTP regions in the three periods (Fig. 5j–u). The q values of humidity show a significant decreasing trend in China in P1-2 (Fig. 5a) and P2 (Fig. 5c). Similarly, decreasing trends are observed in MTH, NS, and WTH regions in P1-2 and P2, and an increasing trend in P1 (Fig. 5d–l). In NWA and QTP regions, the q values show a decreasing trend in the three periods (Fig. 5p–u).

3.3.3. Thermal conditions

Generally, the controlling effect of temperature for the NDVI distribution shows a decreasing trend in most regions during 1982–2015, except for the WTH region (Fig. 6). In China, the q values of mean temperature, maximum temperature, and minimum temperature showed decreasing trends in P1-2 and P2 (Fig. 6a, c). The q values of mean temperature decrease in MTH and NWA, and increase in WTH during the three periods (Fig. 6d–f, p–r, j–l). The q values of mean temperature show a decreasing trend in P1-2 and P1 (Fig. 6s, t), and an increasing trend in P2 in QTP (Fig. 6u). The q value of maximum temperature shows a decreasing trend in China, MTH, and STH regions during the three periods (Fig. 6a–f, m–o) and a decreasing trend in P1-2, an increasing trend in P1 and a decreasing trend in P2 in NS and NWA (Fig. 6g–i, p–r). In QTP, the q value of maximum temperature increases in P1-2 and P2 (Fig. 6s, u) but decreases in P1 (Fig. 6t). The q values of minimum temperature show an increasing trend in WTH but decreasing trends in the other regions in P1-2 (Fig. 6). The q value of wind speed shows decreasing trends in China in the three periods (Fig. 6a–c), a similar phenomenon is seen in regions of MTH, STH, NWA and QTP (Fig. 6d–f, m–u).

3.3.4. Anthropogenic factors

Land use change and human populations can be viewed as significantly important anthropogenic factors in vegetation change (Lü et al., 2015; Chen et al., 2019). In this study, land use type and population density were chosen as anthropogenic factors to detect their strength of spatial association with NDVI. Due to data availability and continuity, we only calculated the q values of land use type for the year of 1982, 1990, 1995, 2000 and 2015, and the q values of population for the period during 2000–2015. The results show that the q values of anthropogenic factors represent different changing trends for the NDVI distribution in different regions. The q values of land use type show a decreasing trend in China and WTH, and an increasing trend in MTH, NS, STH, NWA and QTP regions during 1982–2015 (Fig. 7a). The q values of population show an increasing trend in China and most ecological regions, including MTH, NS, WTH, and NWA regions (Fig. 7b).

Table 2
Dominant interaction factors and its q values in different regions.

	P1-2		P1		P2	
MTH	Pre ∩ Elevation	0.694	Pre ∩ Elevation	0.647	Pre ∩ Elevation	0.704
NS	Pre ∩ Tmax	0.675	Pre ∩ Tmean	0.705	Pre ∩ Tmax	0.647
WTH	Humidity ∩ Elevation	0.498	Pre ∩ Elevation	0.464	Pre ∩ Elevation	0.499
STH	Pre ∩ Elevation	0.554	Pre ∩ Elevation	0.534	Pre ∩ Elevation	0.560
NWA	Pre ∩ Land use	0.679	Pre ∩ Land use	0.658	Pre ∩ Land use	0.685
QTP	Pre ∩ Tmax	0.867	Pre ∩ Tmax	0.862	Pre ∩ Tmax	0.870
China	Pre ∩ Elevation	0.912	Pre ∩ Elevation	0.907	Pre ∩ Elevation	0.913

Note: Pre, Tmean and Tmax represent precipitation, mean temperature and maximum temperature, respectively.

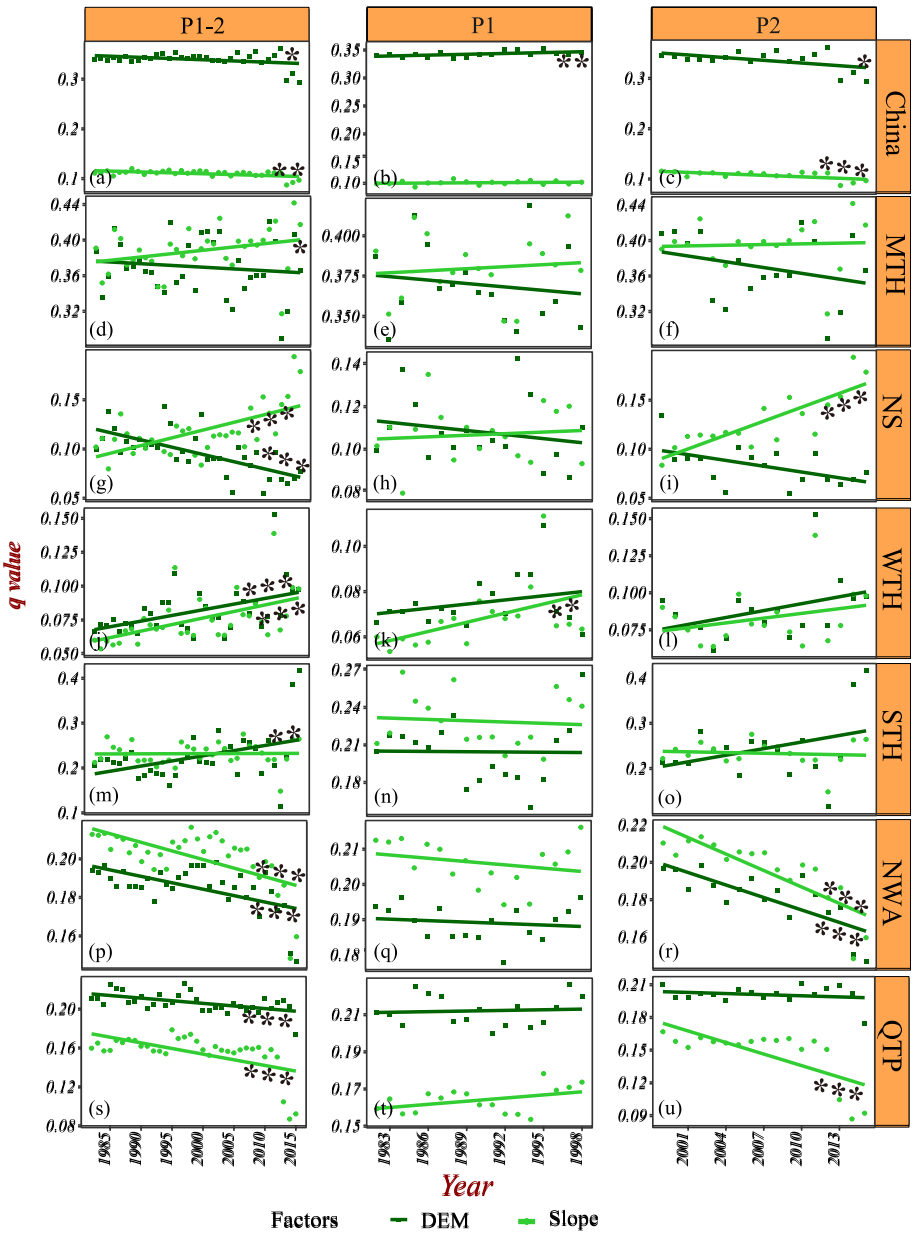

Fig. 4. The temporal dynamics of q values of topographic factors (*** means p-value < 0.01, **means p-value < 0.05, and * means p-value < 0.1).

4. Discussion

4.1. Spatiotemporal variation of vegetation greenness across eco-geographic regions

Vegetation greenness generally increases in national scale over China, but greening and browning vegetation dynamics both exist in China (Liu and Lei, 2015; Chen et al., 2019). In this study, vegetation in China shows increasing variability during three periods; however, heterogeneous regional greenness changes have been observed. The NDVI shows an increasing trend in all regions during 1982–1998, but displays a decreasing trend in NWA and QTP regions during 1999–2015, and an increasing trend in the other regions. Due to the dominant factor for vegetation greenness in these regions was precipitation, followed by humidity, we believed that the reasons for the browning trend may be caused by the weakening water conditions, for example, the humidity displayed significant decreasing trends in NWA and QTP regions. In addition, precipitation showed decreasing trend in QTP region with the slope of −3.641 (mm/a), non-significant increasing trend with slope of 0.547 (mm/a) in NWA region; on the contrary, precipitation showed significant rising trend in other regions (Table S2). Another reason may be that at the scale of AVHRR it is difficult to see details in these regions because of the strong background of soil (Piao et al., 2020), while at the scale of MODIS it is easier to pick fine details in vegetation. For instance, browning trend was detected from AVHRR dataset since 2000s (de Jong et al., 2012), but MODIS C6 data which was calibrated better and could identify vegetation from background precisely, showed an overall greening trend on the contrary (Piao et al., 2020). In this study, we focused on the spatial consistency and strength of association between factors and NDVI; the temporal changing trend of NDVI in each grid played little role in the identification of dominant factors in the spatial scale.

Spatially stratified heterogeneity, with elevation and slope as stratification variables, shows diverse changing trends across different eco-geographic regions. For example, the q values of elevation show an increasing trend in warmer regions (WTH and STH regions) but a decreasing trend in cooler regions, including NWA, QTP, NS, and MTH regions. That is caused by the different response of vegetation to

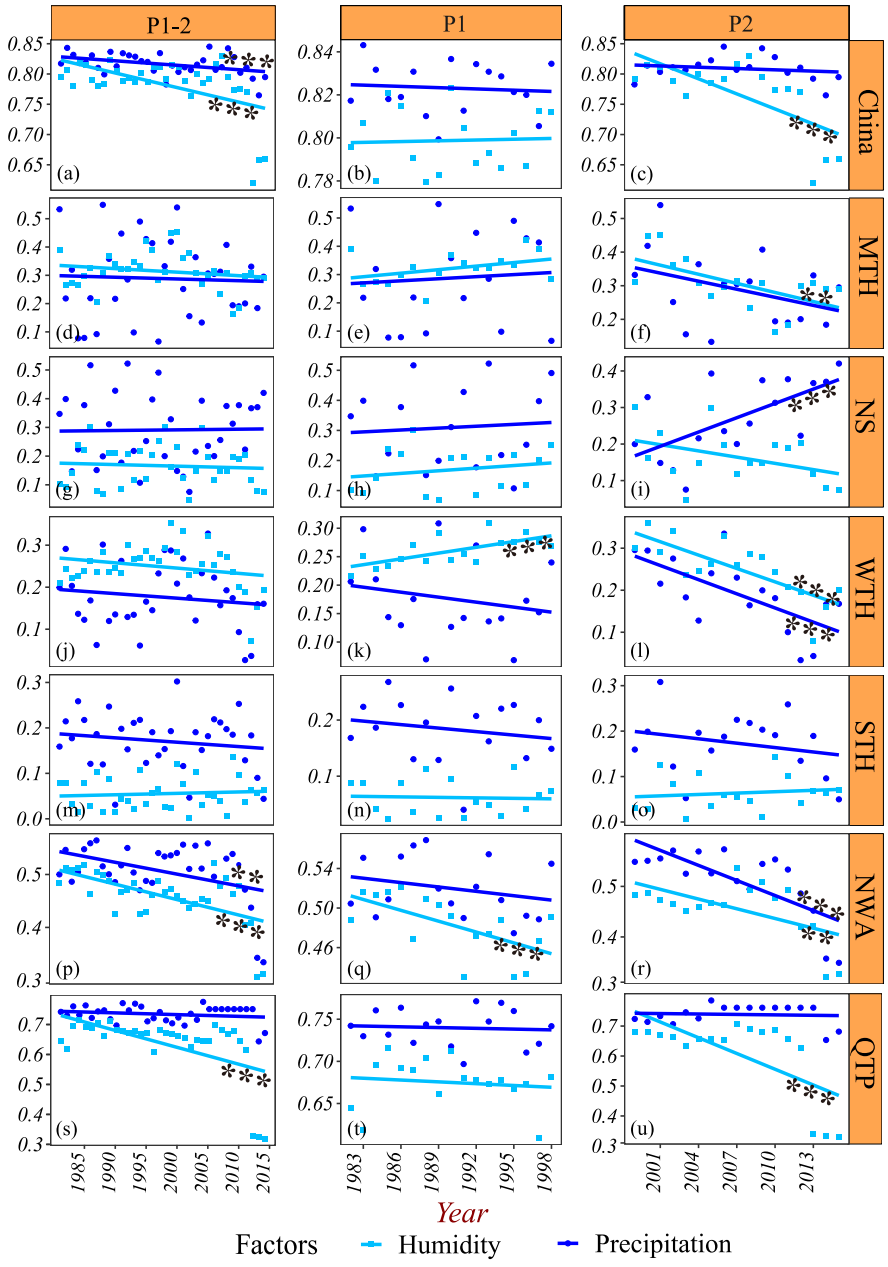

Fig. 5. The temporal dynamic of q values of water conditions (*** means p-value < 0.01, **means p-value < 0.05, * means p-value < 0.1).

environmental factors in different regions. For example, in cooler regions in this study, including NWA, QTP, NS and MTH regions, cooler locations are suggested to warm faster than warmer ones and the greening of the land surface in cold regions are consistent with recent global warming, raising concerns of a more homogenized landscape of changes in vegetation because of global warming along elevation (Gao et al., 2019; Keenan and Riley, 2018), thus the spatial heterogeneity along an altitudinal gradient decreases. On the contrary, in the tropics and subtropics, including WTH and STH regions, where vegetation often grows near its thermal optimum, temperature is not the dominant limiting factor for vegetation growth (Corlett, 2011; Doughty and Goulden, 2008); in contrast, low temperatures at high elevation may actually constrain respirational carbon losses and reduce evapotranspiration demand, leading to enhanced vegetation growth and greenness. Furthermore, in most temperate regions, increasing precipitation may contribute to increasing spatial heterogeneity of NDVI along an elevation, particularly increasing precipitation along an elevation facilitated vegetation growth in high elevation areas (Kharuk et al., 2008; Deng et al., 2013). Precipitation showed increasing trend in both P1 and P2 periods in STH and WTH regions (Table S2). Thus, in STH and WTH regions, the q values of elevation increase.

4.2. Identification and temporal dynamics of drivers for NDVI

There have been considerable efforts made in understanding the mechanisms and drivers of vegetation greening. In this study, generally, precipitation is the dominant climatic factor for NDVI, with the highest strength of association in China and most eco-geographic regions. However, some studies have found that temperature plays a more important role than precipitation in vegetation greenness (Richardson et al., 2013; Zhang et al., 2018). There are two potential reasons why the strength of association between precipitation and NDVI are higher than that of temperature. One reason is that during the long-term evolution of terrestrial ecosystems, vegetation is widely distributed across China and

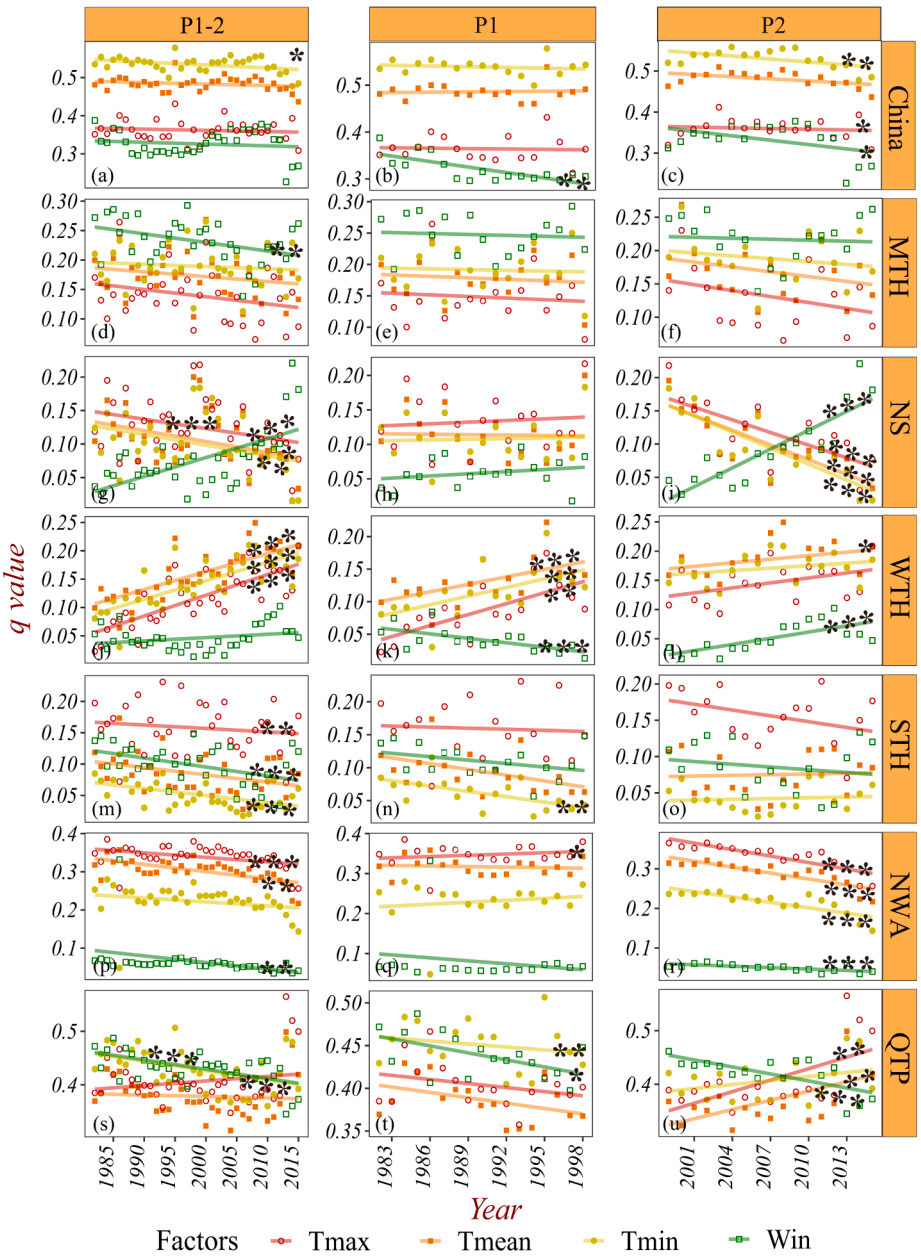

Fig. 6. Temporal dynamics of *q* values of thermal factors (*** means *p*-value < 0.01, ** means *p*-value < 0.05, * means *p*-value < 0.1).

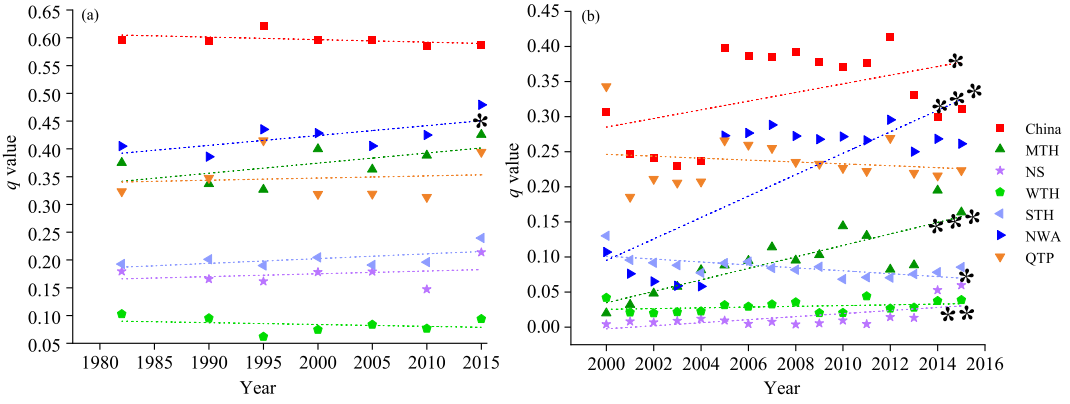

Fig. 7. The temporal dynamic of *q* value of anthropogenic factors, (a) land use type, and (b) population density (*** means *p*-value < 0.01, **means *p*-value < 0.05, * means *p*-value < 0.1).

is adapted well to temperature through an adjustment of the structure or spatial distribution of vegetation (Lenoir et al., 2008). In addition, in water-stressed regions, such as arid and semi-arid areas, there is a significant difference of vegetation type and greenness under diverse water conditions (Chen and Ren, 2013; Zhu et al., 2020). Another reason is that temperature rise affects vegetation growth in two different ways: moderate warming can promote vegetation growth by improving photosynthetic efficiency (Wang et al., 2015), but high temperature can enhance water consumption of vegetation, intensify drought and accelerate the denaturation of enzymes in some plants, resulting in inhibiting vegetation growth (Zhang et al., 2015; Yan et al., 2019). Thus, the strength of association between temperature and NDVI is lower than that of precipitation for the strength of association with NDVI.

The explanatory power of drivers differed in diverse eco-geographic regions. For example, mean temperature owed the highest strength of association (q value of 0.377 in P1-2) in the coolest region, namely QTP region where the mean temperature is −1.66℃, while in the hottest region (STH region with mean temperature of 16.00℃), the strength of association between temperature and NDVI was only 0.099 in P1-2. The reason was that temperature was not the growth limiting factor in tropic regions, thus temperature played little role in the spatial distribution of NDVI. On the contrary, temperature is the most important factor to decide vegetation growth in cold regions. Similarly, precipitation played a more important role in arid and semi-arid regions, which reached the highest strength of association in QTP region (0.772 in P1-2), followed by NWA region (0.547 in P1-2), while in the humid and sub-humid regions, including STH and WTH regions, the strength of association between precipitation and NDVI had its lowest value, with the q value of 0.243 and 0.268, respectively. These results illustrated that vegetation growth was significantly influenced by the limiting environmental factor, which is consistent with the theory of Liebig's law of the minimum (Stine and Huybers, 2017).

A decreasing strength of association between NDVI and temperature was also found in this study, with the q values decreasing across China over the past 34 years, which is in line with previous publications (Fu et al., 2015; Keenan and Riley, 2018). Keenan and Riley (2018) identified a decrease in the temperature limitation of vegetation, with a 16.4% decrease in the area of vegetation land limited by temperature over the past 30 years; the contribution of rising temperature to the enhanced greening trend will weaken or even disappear under continued global warming (Piao et al., 2006). Although the limiting effect of temperature for vegetation is observed in China, the response of vegetation to temperature may be heterogeneous in different eco- geographic regions. We found that strength of association between temperature and NDVI displayed decreasing trends in five eco-geographic regions with diverse variability but increased in WTH regions. Similarly, the trends of the controlling effect of water conditions and human activities varied across different regions. A possible mechanism underlying the varying trends is that the impact of environmental change on vegetation greenness and vegetation sensitivity to external disturbance varies across regions (Zhu et al., 2016; Piao et al., 2020); spatially heterogeneous temperature rising and human disturbances may play diverse roles over different eco-geographic regions, thus causing the spatially heterogeneous response of vegetation to external environmental changes.

We stress that our method itself finds strength of association between factors and vegetation greenness in space, but not causations for temporal change. The input data for the GeoDetector method were categorical variables, the continuous datasets (including, for example, climatic factors) were separated into several categories, which makes the strength of association comparable among categorical factors and continuous factors (Luo et al., 2016), and the inter-annual variation in each grid cell was largely ignored. This method belongs to the category of analysis of variance without the linear hypothesis in the relationship between two variables, and the interaction detector identify the real interaction effect compared with the multiplicative interactions presupposed by econometrics. Thus, the results based on GeoDetector is more reliable than classical regression analysis (Wang and Xu, 2017). For historical reasons, we believe that the spatial distribution and differentiation of vegetation greenness represent the long-term adaption of vegetation to external factors, including environmental factors and anthropogenic factors (Lenoir et al., 2008). The identification of high spatial association factors helps considerably in identifying causality. Our quantitative assessment of these dominant factors confirms not only their relative importance but also that the temporal dynamics of strength of association between the factors and NDVI differed in space and time.

4.3. Limitations and future studies

Some uncertainties remain in understanding the identification and temporally changing dynamics of the drivers for vegetation in China. First, the uncertainties of identification of dominant drivers may include factors not considered, such as CO_2 fertilisation effect (Piao et al., 2015), anthropogenic disturbance (e.g. afforestation and deforestation), insects (Kurz et al., 2008) and wildfire (Beck and Goetz, 2012). Second, the data quality was restricted by data availability; e.g., climate data were acquired from the National Meteorological Information Center dataset, which were interpolated from meteorological station records. Considerable errors may arise from the sparse distribution of meteorological stations, especially in QTP region. However, despite several uncertainties, our study identified the relative importance of drivers across spatiotemporal scales and provided evidence of an overall decrease in the strength of association among vegetation and hydrothermal factors. This study also identified an increase in the correlation between vegetation and anthropogenic activities. Our findings provide a reference for terrestrial ecosystem management. We suggest that further study should focus on a deep analysis of temporal variation and spatial heterogeneity of driving mechanism for vegetation greening or browning trends. Additionally, in the future experiment design and vegetation model simulation, the human activity should be more significantly considered.

5. Conclusion

Our study identified the spatiotemporal differentiation on the response of vegetation greenness to climate change and land cover change in six eco-geographic regions across China. Our findings will help to enable decision-makers to effectively manage and develop sustainable ecosystems by comprehensively considering the regional and temporal differences of vegetation greenness and its drivers across diverse sub-regions. The primary conclusions are summarized as follows:

(1) Vegetation greenness changes significantly across space and time. Vegetation represents a greening trend in the six eco-geographic regions during 1982–1998, but greening and browning both exist during 1999–2015. In addition, due to the diverse response of vegetation to climatic factors in different eco-geographic regions, the spatial heterogeneity along an elevation gradient displays opposite changing trend with weakening trend in colder regions (including NWA, QTP, NS and MTH) and enhancing trend in warmer regions, including STH and WTH regions.
(2) The dominant factors for NDVI and the spatial association between NDVI and factors are heterogeneous in the six eco-geographic regions of China. Water conditions are the dominant factor for landscape variation of NDVI across China; the strength of association between water conditions and NDVI is higher in arid and semi-arid areas compared with humid areas. The dominant factors differ across the six eco-geographic regions; e.g., topographic factors dominate in the MTH region, and precipitation dominates in the NS, NWA and QTP regions.
(3) Generally, the strength of association between hydrothermal factors and NDVI decreases, but the linkages between human

activities and NDVI are enhanced. Meanwhile, the temporal dynamics of strength of association between factors and NDVI vary in different time series and regions. For instance, the strength of association between wind speed and NDVI decrease during 1982–1998, but increase during 1999–2015 in the WTH region; in contrast there are decreasing trends in the QTP region in both periods.

Declaration of Competing Interest

The authors declare that they have no known competing financial interests or personal relationships that could have appeared to influence the work reported in this paper.

Acknowledgements

We would like to thank the financial support provided by the National Key Research and Development Plan of China [grant number: 2019YFA0606602].

Funding

This study was supported by the National Key Research and Development Plan of China [grant number: 2019YFA0606602].

Author contribution statement

Huan Wang designed and wrote this paper, Shijie Yan, Ze Liang, Kewei Jiao, Delong Li, Feili Wei and Shuangcheng Li provided a lot of valuable suggestions for the improvement of the paper.

Appendix A. Supplementary data

Supplementary data to this article can be found online at https://doi.org/10.1016/j.ecolind.2021.107831.

References

Beck, P.S.A., Goetz, S.J., 2012. Satellite observations of high northern latitude vegetation productivity changes between 1982 and 2008: ecological variability and regional differences. Environ. Res. Lett. 7 (2) https://doi.org/10.1088/1748-9326/7/2/029501.

Bonan, G.B., 2008. Forests and climate change: forcings, feedbacks, and the climate benefits of forests. Science 320 (5882), 1444–1449.

Buitenwerf, R., Bond, W.J., Stevens, N., Trollope, W.S.W., 2012. Increased tree densities in South African savannas: > 50 years of data suggests CO2 as a driver. Glob. Change Biol. 18 (2), 675–684. https://doi.org/10.1111/j.1365-2486.2011.02561.x.

Cai, D., Fraedrich, K., Sielmann, F., Guan, y., Guo, S., 2016. Land-cover characterization and aridity changes of South America (1982-2006): an attribution by ecohydrological diagnostics. J. Clim. 29(22), 8175–8189.

Cai, D., Fraedrich, K., Sielmann, F., Zhang, L., Zhu, X., Guo, S., Guan, Y., 2015. Vegetation dynamics on the Tibetan Plateau (1982–2006): an attribution by ecohydrological diagnostics. J. Clim. 28 (11), 4576–4584.

Chen, C., Park, T., Wang, X., Piao, S., Xu, B., Chaturvedi, R.K., Fuchs, R., Brovkin, V., Ciais, P., Fensholt, R., Tømmervik, H., Bala, G., Zhu, Z., Nemani, R.R., Myneni, R.B., 2019. China and India lead in greening of the world through land-use management. Nat. Sustainability 2 (2), 122–129. https://doi.org/10.1038/s41893-019-0220-7.

Chen, H., Ren, Z., 2013. Response of vegetation coverage to changes of precipitation and temperature in Chinese Mainland. Bull. Soil Water Conserv. 33 (2), 78–82. https://doi.org/10.13961/j.cnki.stbctb.2013.02.001.

Corlett, R.T., 2011. Impacts of warming on tropical lowland rainforests. Trends Ecol. Evol. 26 (11), 606–613.

Jong, R., Verbesselt, J., Schaepman, M.E., Bruin, S., 2012. Trend changes in global greening and browning: contribution of short-term trends to longer-term change. Glob. Change Biol. 18 (2), 642–655.

Deng, S.-f., Yang, T.-B., Zeng, B., Zhu, X.-F., Xu, H.-J., 2013. Vegetation cover variation in the Qilian Mountains and its response to climate change in 2000–2011. J. Mountain Sci. 10 (6), 1050–1062.

Doughty, C.E., Goulden, M.L., 2008. Are tropical forests near a high temperature threshold. J. Geophys. Res. 113 (G1), n/a–n/a. https://doi.org/10.1029/2007JG000632.

Du, Z., Zhang, X., Xu, X., Zhang, H., Wu, Z., Pang, J., 2017. Quantifying influences of physiographic factors on temperate dryland vegetation, Northwest China. Sci. Rep. 7 (1), 1–9. https://doi.org/10.1038/srep40092.

Fensholt, R., Langanke, T., Rasmussen, K., Reenberg, A., Prince, S.D., Tucker, C., Scholes, R.J., Le, Q.B., Bondeau, A., Eastman, R., Epstein, H., Gaughan, A.E., Hellden, U., Mbow, C., Olsson, L., Paruelo, J., Schweitzer, C., Seaquist, J., Wessels, K., 2012. Greenness in semi-arid areas across the globe 1981–2007 - an Earth Observing Satellite based analysis of trends and drivers. Remote Sens. Environ. 121, 144–158. https://doi.org/10.1016/j.rse.2012.01.017.

Fu, B., Wang, S., Liu, Y., Liu, J., Liang, W., Miao, C., 2017. Hydrogeomorphic ecosystem responses to natural and anthropogenic changes in the loess Plateau of China. Annu. Rev. Earth Planet. Sci. 45 (1), 223–243. https://doi.org/10.1146/annurev-earth-063016-020552.

Fu, Y., Zhao, H., Piao, S., Peaucelle, M., Peng, S., Zhou, G., Ciais, P., Huang, M., Menzel, A., Uelas, J.P., Song, Y., Vitasse, Y., Zeng, Z., Janssens, I.A., 2015. Declining global warming effects on the phenology of spring leaf unfolding. Nature 526 (7571), 104–107.

Gao, J., Jiao, K., Wu, S., Ma, D., Zhao, D., Yin, Y., Dai, E., 2017. Past and future effects of climate change on spatially heterogeneous vegetation activity in China. Earth's Future 5 (7), 679–692.

Gao, J., Wang, H., 2019. Temporal analysis on quantitative attribution of karst soil erosion: a case study of a peak-cluster depression basin in Southwest China. Catena 172, 369–377.

Gao, M., Piao, S., Chen, A., Yang, H., Liu, Q., Fu, Y.H., Janssens, I.A., 2019. Divergent changes in the elevational gradient of vegetation activities over the last 30 years. Nat. Commun. 10 (1), 1–10. https://doi.org/10.1038/541467-019-11035-W.

Hsu, J.S., Powell, J., Adler, P.B., 2012. Sensitivity of mean annual primary production to precipitation. Glob. Change Biol. 18 (7), 2246–2255.

Huang, K., Xia, J., Wang, Y., Ahlström, A., Chen, J., Cook, R.B., Cui, E., Fang, Y., Fisher, J.B., Huntzinger, D.N., Li, Z., Michalak, A.M., Qiao, Y., Schaefer, K., Schwalm, C., Wang, J., Wei, Y., Xu, X., Yan, L., Bian, C., Luo, Y., 2018. Enhanced peak growth of global vegetation and its key mechanisms. Nat. Ecol. Evol. 2 (12), 1897–1905.

Huang, S., Zheng, X., Ma, L., Wang, H., Huang, Q., Leng, G., Meng, E., Guo, Y.i., 2020. Quantitative contribution of climate change and human activities to vegetation cover variations based on GA-SVM model. J. Hydrol. 584, 124687. https://doi.org/10.1016/j.jhydrol.2020.124687.

Huxman, T.E., Smith, M.D., Fay, P.A., Knapp, A.K., Shaw, M.R., Loik, M.E., Smith, S.D., Tissue, D.T., Zak, J.C., Weltzin, J.F., Pockman, W.T., Sala, O.E., Haddad, B.M., Harte, J., Koch, G.W., Schwinning, S., Small, E.E., Wlliams, D.G., 2004. Convergence across biomes to a common rain-use efficiency. Nature 429 (6992), 651–654.

Kalisa, W., Igbawua, T., Henchiri, M., Ali, S., Zhang, S., Bai, Y., Zhang, J., 2019. Assessment of climate impact on vegetation dynamics over East Africa from 1982 to 2015. Sci. Rep. 9, 20. https://doi.org/10.1038/s41598-019-53150-0.

Keenan, T.F., Riley, W.J., 2018. Greening of the land surface in the world's cold regions consistent with recent warming. Nat. Clim. Change 8 (9), 825–828.

Kharuk, V.I., Dvinskaya, M.L., Im, S.T., Ranson, K.J., 2008. Tree vegetation of the forest-tundra ecotone in the Western Sayan mountains and climatic trends. Russ. J. Ecol. 39 (1), 8–13.

Krishnaswamy, J., John, R., Joseph, S., 2014. Consistent response of vegetation dynamics to recent climate change in tropical mountain regions. Glob. Change Biol. 20 (1), 203–215.

Kurz, W.A., Dymond, C.C., Stinson, G., Rampley, G.J., Safranyik, L., 2008. Mountain pine beetle and forest carbon feedback to climate change. Nature 452 (7190), 987–990.

Lenoir, J., Gegout, J.C., Marquet, P.A., de Ruffray, P., Brisse, H., 2008. A significant upward shift in plant species optimum elevation during the 20th century. Science 320 (5884), 1768–1771. https://doi.org/10.1126/science.1156831.

Leverkus, A.B., Murillo, P.G., Dona, V.J., Pausas, J.G., 2019. Wildfires: opportunity for restoration? Science 363 (6423), 134–135.

Liu, Y., Lei, H., 2015. Responses of natural vegetation dynamics to climate drivers in China from 1982 to 2011. Remote Sensing 7 (8), 10243–10268.

Luo, W., Jasiewicz, J., Stepinski, T., Wang, J., Xu, C., Cang, X., 2016. Spatial association between dissection density and environmental factors over the entire conterminous United States. Geophys. Res. Lett. 43 (2), 692–700. https://doi.org/10.1002/grl.v43.210.1002/2015GL066941.

Lü, Y., Zhang, L., Feng, X., Zeng, Y., Fu, B., Yao, X., Li, J., Wu, B., 2015. Recent ecological transitions in China: greening, browning, and influential factors. Sci. Rep. 5 (1), 8732.

Nemani, R.R., Keeling, C.D., Hashimoto, H., Jolly, W.M., Piper, S.C., Tucker, C.J., Myneni, R.B., Running, S.W., 2003. Climate-driven increases in global terrestrial net primary production from 1982 to 1999. Science 300 (5625), 1560–1563. https://doi.org/10.1126/science.1082750.

Niinemets, U., Flexas, J., Penuelas, J., 2011. Evergreens favored by higher responsiveness to increased CO2. Trends Ecol. Evol. 26 (3), 136–142. https://doi.org/10.1016/j.tree.2010.12.012.

Piao, S., Friedlingstein, P., Ciais, P., Zhou, L., Chen, A., 2006. Effect of climate and CO2 changes on the greening of the Northern Hemisphere over the past two decades. Geophys. Res. Lett. 33 (23) https://doi.org/10.1029/2006gl028205.

Piao, S., Nan, H., Huntingford, C., Ciais, P., Friedlingstein, P., Sitch, S., Peng, S.S., Ahlstrom, A., Canadell, J.G., Cong, N., Levis, S., Levy, P.E., Liu, L.L., Lomas, M.R., Mao, J.F., Myneni, R.B., Peylin, P., Poulter, B., Shi, X., Yin, G., Viovy, N., Wang, T., Wang, X., Zaehle, S., Zeng, N., Zeng, Z., Chen, A., 2014. Evidence for a weakening relationship between interannual temperature variability and northern vegetation activity. Nat. Commun. 5 (1), 5018.

Piao, S., Wang, X., Ciais, P., Zhu, B., Wang, T., Liu, J., 2011. Changes in satellite-derived vegetation growth trend in temperate and boreal Eurasia from 1982 to 2006. Glob. Change Biol. 17 (10), 3228–3239. https://doi.org/10.1111/j.1365-2486.2011.02419.x.

Piao, S., Wang, X., Park, T., Chen, C., Lian, X., He, Y., Bjerke, J.W., Chen, A., Ciais, P., Tommervik, H., Nemani, R.R., Myneni, R.B., 2020. Characteristics, drivers and feedbacks of global greening. https://doi.org/10.1038/s43017-019-0001-x.

Piao, S., Yin, G., Tan, J., Cheng, L., Huang, M., Li, Y., Liu, R., Mao, J., Myneni, R.B., Peng, R., Poulter, B., Shi, X., Xiao, Z., Zeng, N., Zeng, Z., Wang, Y., 2015. Detection and attribution of vegetation greening trend in China over the last 30 years. Glob. Change Biol. 21 (4), 1601–1609.

Qu, L., Huang, Y., Yang, L., Li, Y., 2020. Vegetation restoration in response to climatic and anthropogenic changes in the Loess Plateau, China. Chin. Geogr. Sci. 30 (1), 89–100.

Richardson, A.D., Keenan, T.F., Migliavacca, M., Ryu, Y., Sonnentag, O., Toomey, M., 2013. Climate change, phenology, and phenological control of vegetation feedbacks to the climate system. Agric. For. Meteorol. 169, 156–173.

Song, X., Hansen, M., Stehman, S., Potapov, P., Tyukavina, A., Vermote, E., Townshend, J., 2018. Global land change from 1982 to 2016.". Nature 563 (7732), E26.

Sun, J., Wang, X., Chen, A., Ma, Y., Cui, M., Piao, S., 2011. NDVI indicated characteristics of vegetation cover change in China's metropolises over the last three decades. Environ. Monit. Assess. 179 (1–4), 1–14. https://doi.org/10.1007/s10661-010-1715-x.

Stine, A.R., Huybers, P., 2017. Implications of Liebig's law of the minimum for tree-ring reconstructions of climate. Environ. Res. Lett. 12 (11), 114018. https://doi.org/10.1088/1748-9326/aa8cd6.

Tao, J., Zhang, Y., Dong, J., Fu, Y.u., Zhu, J., Zhang, G., Jiang, Y., Tian, L.i., Zhang, X., Zhang, T., Xi, Y.i., 2015. Elevation-dependent relationships between climate change and grassland vegetation variation across the Qinghai-Xizang Plateau. Int. J. Climatol. 35 (7), 1638–1647. https://doi.org/10.1002/joc.2015.35.issue-710.1002/joc.4082.

Toms, J.D., Lesperance, M.L., 2003. Piecewise regression: a tool for identifying ecological thresholds. Ecology 84 (8), 2034–2041. https://doi.org/10.1890/02-0472.

Wang, C., Guo, H., Zhang, L.i., Liu, S., Qiu, Y., Sun, Z., 2015. Assessing phenological change and climatic control of alpine grasslands in the Tibetan Plateau with MODIS time series. Int. J. Biometeorol. 59 (1), 11–23.

Wang, H., Gao, J., Hou, W., 2018. Quantitative attribution analysis of soil erosion in different morphological types of geomorphology in karst areas: based on the geographical detector method. Acta Geographica Sinica 73 (9), 1674–1686 (in Chinese).

Wang, J.-F., Li, X.-H., Christakos, G., Liao, Y.-L., Zhang, T., Gu, X., Zheng, X.-Y., 2010. Geographical detectors-based health risk assessment and its application in the neural tube defects study of the Heshun Region, China. Int. J. Geogr. Inform. Sci. 24 (1), 107–127.

Wang, J., Wang, H., Cao, Y., Bai, Z., Qin, Q., 2016a. Effects of soil and topographic factors on vegetation restoration in opencast coal mine dumps located in a loess area. Sci. Rep. 6 (1), 22058.

Wang, J., Xu, C., 2017. Geodetector: principle and prospective. Acta Geographica Sinica 72 (1), 116–134 (in Chinese).

Wang, J., Zhang, T., Fu, B., 2016b. A measure of spatial stratified heterogeneity. Ecol. Ind. 67, 250–256. https://doi.org/10.1016/j.ecolind.2016.02.-052.

Wang, X., Piao, S., Ciais, P., Li, J., Friedlingstein, P., Koven, C., Chen, A., 2011. Spring temperature change and its implication in the change of vegetation growth in North America from 1982 to 2006. PNAS 108 (4), 1240–1245.

Wei, F., Liang, Z.e., Wang, Y., Huang, Z., Wang, H., Sun, F., Li, S., 2020. Exploring the driving factors of the spatiotemporal variation of precipitation in the Jing–Jin–Ji urban agglomeration from 2000 to 2015. Sustainability 12 (18), 7426. https://doi.org/10.3390/su12187426.

Wu, S., Yin, Y., Zhao, D., Huang, M., Shao, X., Dai, E., 2010. Impact of future climate change on terrestrial ecosystems in China. Int. J. Climatol. 30 (6), 866–873.

Xiao, J., Moody, A., 2005. Geographical distribution of global greening trends and their climatic correlates: 1982–1998. Int. J. Remote Sens. 26 (11), 2371–2390.

Xu, J., Yin, R., Li, Z., Liu, C., 2006. China's ecological rehabilitation: unprecedented efforts, dramatic impacts, and requisite policies. Ecol. Econ. 57 (4), 595–607.

Yan, S., Wang, H., Jiao, K., 2019. Spatiotemporal dynamic of NDVI in the Beijing-Tianjin-Hebei region based on MODIS data and quantitative attribution. J. Geo-inform. Sci. 21 (5), 767–780 (in Chinese).

Yang, Y., Fang, J., Ma, W., Wang, W., 2008. Relationship between variability in aboveground net primary production and precipitation in global grasslands. Geophys. Res. Lett. 35 (23) https://doi.org/10.1029/2008gl035408.

Zhang, K., Kimball, J.S., Nemani, R.R., Running, S.W., Hong, Y., Gourley, J.J., Yu, Z., 2015. Vegetation greening and climate change promote multidecadal rises of global land evapotranspiration. Sci. Rep. 5 (1) https://doi.org/10.1038/srep15956.

Zhang, P., Cai, Y., Yang, W., Yi, Y., Yang, Z., Fu, Q., 2020a. Contributions of climatic and anthropogenic drivers to vegetation dynamics indicated by NDVI in a large dam-reservoir-river system. J. Cleaner Prod. 256, 120477. https://doi.org/10.1016/j.jclepro.2020.120477.

Zhang, W., Wang, L., Xiang, F., Qin, W., Jiang, W., 2020b. Vegetation dynamics and the relations with climate change at multiple time scales in the Yangtze River and Yellow River Basin, China. Ecol. Indic. 110, 105892. https://doi.org/10.1016/j.ecolind.2019.105892.

Zhang, Y., Wang, X., Li, C., Cai, Y., Yang, Z., Yi, Y., 2018. NDVI dynamics under changing meteorological factors in a shallow lake in future metropolitan, semiarid area in North China. Sentific Rep. 8 (1) https://doi.org/10.1038/s41598-018-33968-w.

Zhao, D., Wu, S., 2014. Vulnerability of natural ecosystem in China under regional climate scenarios: an analysis based on eco-geographical regions. J. Geog. Sci. 24 (2), 237–248.

Zhao, H., Wu, R., Hu, J., Yang, F., Wang, J., Guo, Y., Zhou, J., Wang, Y., Zhang, C., Feng, Z., 2020. The contrasting east-west pattern of vegetation restoration under the large-scale ecological restoration programmes in southwest China. Land Degrad. Dev. 31 (13), 1688–1698. https://doi.org/10.1002/ldr.v31.1310.1002/ldr.3520.

Zhao, Z., Liu, J., Peng, J., Li, S., Wang, Y., 2015. Nonlinear features and complexity patterns of vegetation dynamics in the transition zone of North China. Ecol. Ind. 49, 237–246.

Zheng, D., 2008. Chinese eco-geographical regionalization research. The Commercial Press, Beijing (in Chinese).

Zhou, L.M., Tucker, C.J., Kaufmann, R.K., Slayback, D., Shabanov, N.V., Myneni, R.B., 2001. Variations in northern vegetation activity inferred from satellite data of vegetation index during 1981 to 1999. J. Geophys. Res.-Atmos. 106 (D17), 20069–20083. https://doi.org/10.1029/2000jd000115.

Zhu, L., Meng, J., Zhu, L., 2020. Applying Geodetector to disentangle the contributions of natural and anthropogenic factors to NDVI variations in the middle reaches of the Heihe River Basin. Ecol. Ind. 117, 106545. https://doi.org/10.1016/j.ecolind.2020.106545.

Zhu, Z., Piao, S., Myneni, R.B., Huang, M., Zeng, Z., Canadell, J.G., Ciais, P., Sitch, S., Friedlingstein, P., Arneth, A., Cao, C., Cheng, L., Kato, E., Koven, C., Li, Y., Lian, X.u., Liu, Y., Liu, R., Mao, J., Pan, Y., Peng, S., Peñuelas, J., Poulter, B., Pugh, T.A.M., Stocker, B.D., Viovy, N., Wang, X., Wang, Y., Xiao, Z., Yang, H., Zaehle, S., Zeng, N., 2016. Greening of the Earth and its drivers. Nat. Clim. Change 6 (8), 791–795.